

The light output-current characteristics for a laser with the 350 $\mu$ m long electrode and a high-reflection (HR) coated rear facet are shown in Fig. 4. Threshold currents were 6.5 and 22.2mA at 25 and 85°C, respectively. The characteristic temperature between 25 and 50°C was 54K. We obtained light output over 10mW even at 100°C and CW operation up to 120°C. This is the highest temperature operation reported for spot-size transformer integrated lasers to our knowledge. The slope efficiency was 0.38mW/mA at 25°C and 0.26mW/mA at 85°C. The degradation of the efficiency between these two temperatures was only 1.6dB. These characteristics were comparable to those of conventional lasers. Fig. 5 shows the measured far-field pattern of the rear facet HR coated laser. The parallel and vertical FWHM were 9.2 and 10.8°, respectively. These values were  $\sim 1/3$  of that of a conventional laser. Using this laser, we measured the coupling efficiency to a flat ended single-mode fibre for butt-coupling. The coupling efficiency was as high as -3.8dB and the alignment tolerances for 1dB excess loss were  $\pm 2\mu$ m for both parallel and vertical directions when the separation of the laser and the fibre was 10 $\mu$ m. These results show that this laser achieved a narrow beam divergence and a high coupling efficiency to a fibre without deteriorating the threshold current and the temperature dependence.

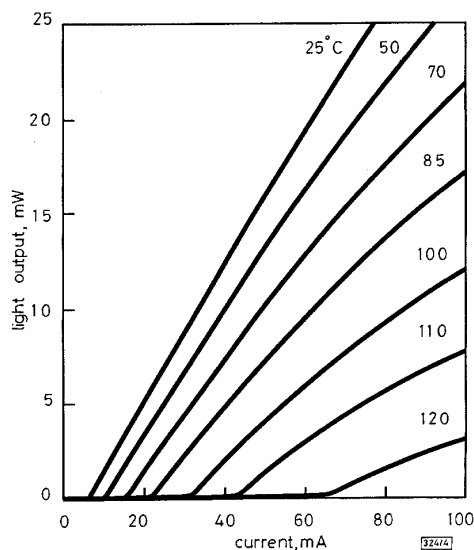


Fig. 4 Light output-current characteristics of laser with HR coated rear facet

Electrode length = 350 $\mu$ m

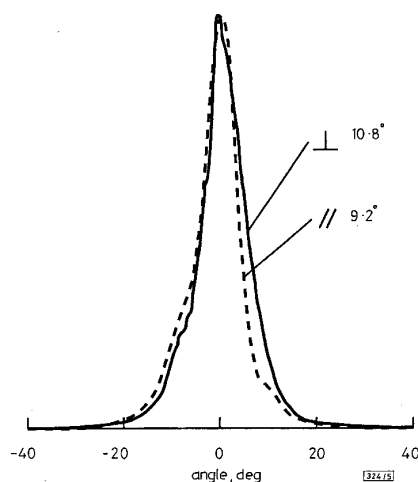


Fig. 5 Far-field-pattern for rear facet HR coated laser at 25°C  
Output power = 10mW

**Summary:** We have demonstrated high temperature operation up to 120°C for 1.3 $\mu$ m narrow beam tapered-thickness waveguide BH MQW lasers. The parallel and vertical far-field FWHM were 9.2

and 10.8°, respectively, and the threshold currents were 6.5mA at 25°C and 22.2mA at 85°C. The coupling efficiency to a flat single-mode fibre was -3.8dB. These good characteristics indicate that this laser is a promising light source for future subscriber transmitter modules.

**Acknowledgments:** We would like to thank Dr. Yamakoshi and Dr. Yamazaki for their encouragement.

© IEE 1995

Electronics Letters Online No: 19951505

31 July 1995

T. Yamamoto, H. Kobayashi, M. Ekawa, T. Fujii, H. Soda and M. Kobayashi (Fujitsu Laboratories Limited, 10-1 Morinosato-Wakamiya, Atsugi 243-01 Japan)

## References

- KOCH, T.L., KOREN, U., EISENSTEIN, G., YOUNG, M.G., ORON, M., GILES, C.R., and MILLER, B.I.: 'Tapered waveguide InGaAs/InGaSP multiple-quantum-well lasers', *IEEE Photonics Technol. Lett.*, 1990, 2, pp. 88-90
- LEALMAN, I.F., SELTZER, C.P., RIVERS, L.J., HARLOW, M.J., and PERRIN, S.D.: 'Low threshold current 1.6 $\mu$ m InGaAs/InP tapered active layer multiquantum well laser with improved coupling to cleaved singlemode fiber', *Electron. Lett.*, 1994, 30, (12), pp. 973-975
- MOERMAN, I., D'HONDT, M., VANDERBAUWHED, W., COUDENYS, G., HAES, J., and DE DOBBELAERE, P.: 'Monolithic integration of a spot size transformer with a planar buried heterostructure InGaAsP/InP-laser using the shadow masked growth technique', *IEEE Photonics Technol. Lett.*, 1994, 6, pp. 888-890
- BEN-MICHAEL, R., KOREN, U., MILLER, B.I., YOUNG, M.G., CHIEN, M., and RAYBON, G.: 'InP-based multiple quantum well lasers with an integrated tapered beam expander waveguide', *IEEE Photonics Technol. Lett.*, 1994, 6, pp. 1412-1414
- KOBAYASHI, H., EKAWA, M., OKAZAKI, N., AOKI, O., OGITA, S., and SODA, H.: 'Tapered thickness MQW waveguide BH MQW lasers', *IEEE Photonics Technol. Lett.*, 1994, 6, pp. 1080-1081
- KOBAYASHI, H., SODA, H., EKAWA, M., OKAZAKI, N., OGITA, S., and YAMAZAKI, S.: 'Narrow beam tapered thickness waveguide integrated BH MQW laser operation at high temperatures'. Dig. 14th IEEE Int. Semicond. Laser Conf., 1994, pp. 191-192
- YAMAMOTO, T., KOBAYASHI, H., EKAWA, M., and SODA, H.: 'Threshold analysis of tapered thickness waveguide BH MQW lasers'. Dig. 10th Int. Conf. Integrated Opt. and Opt. Fibre Commun., 1995, Vol. 3, pp. 112-113

## Measurements of reverse and forward bias absorption and gain spectra in semiconductor laser material

S.D. McDougall and C.N. Ironside

**Indexing terms:** Semiconductor junction lasers, Semiconductor quantum wells

A simple technique for measuring absorption and gain spectra under reverse and forward bias in a two section semiconductor laser is described. Results are presented for an AlGaAs/GaAs multiquantum well laser. For reverse bias, exciton broadening and shifting are observed; and for forward bias, relative gain spectra are measured.

**Introduction:** Gain and absorption measurements in semiconductor laser material can give considerable insight into the operation of the laser and in this Letter we describe a technique for measuring the spectra of semiconductor laser material as a function of biasing conditions. The technique uses a two section semiconductor laser. Multisection semiconductor lasers are employed in various applications. Our group has recently employed multisection lasers for monolithic modelocking of semiconductor lasers [1-4]. These lasers have a saturable absorber section which is simply a reversed biased section of the laser material. To gain a more complete understanding of the operation of the modelocked semi-

conductor laser, we have developed a technique for obtaining the absorption spectrum of the saturable absorber which used the spontaneous emission from the gain section to probe the absorption in the saturable absorber. The technique can simply be adapted for gain by forward biasing the saturable absorber section (described in detail below). To date the measurement of gain spectra of laser material has been a difficult experiment [5–9]. The method presented here is much simpler.

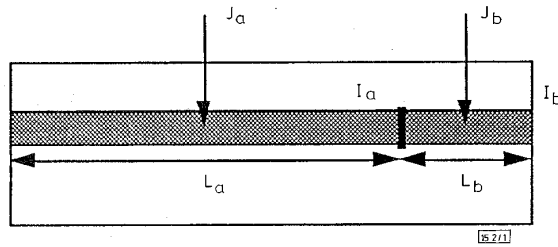


Fig. 1 Layout of two section semiconductor laser used for spectral measurements

The technique is as follows: a two sectioned laser is fabricated using the techniques described in [3, 4]. Fig. 1 is a schematic top view of the device.

The details of the procedure for measuring the gain are given below. We refer to Fig. 1 in which  $J_a$  and  $J_b$  are the current densities in the sections  $a$  and  $b$  which are  $L_a$  and  $L_b$  in length.  $I_a$  is the optical intensity at the end of section  $a$  and  $I_b$  is the optical intensity at the end of section  $b$ , which is also the output. Initially the reference spectrum is measured. Here, the current densities are set at  $J_a = J_b = J_1$  and the output spectrum  $I_{b1}$  is measured over a range of wavelengths. This spectrum contains amplified spontaneous emission from section  $a$ , and some spontaneous emission from section  $b$ ,  $I_{b,spont}(J_1)$ . The complete expression is given by

$$I_{b1} = I_a \exp[-\alpha(J_1)L_b] + I_{b,spont}(J_1)$$

By setting  $J_a = 0$  but keeping  $J_b$  at  $J_1$ ,  $I_{b,spont}(J_1)$  alone is measured. Subtracting these two spectra gives the reference level  $I_{ref}$ .

$$I_{ref} = I_{b1} - I_{b,spont}(J_1)$$

Current density  $J_1$  is chosen to bias the laser approximately at transparency, so we assume that any absorption or gain present is small ( $\alpha \approx 0$ ). If this approximation does not hold (and it may not for all wavelengths) then the measurements are only relative to our  $I_{ref}$ . Also the measurements are not sensitive to losses such as scattering loss that do not change with biasing. Therefore we refer here to change in absorption in the spectra.

To measure the absorption coefficient at some current density  $J_k$  relative to the reference level  $I_{ref}$ ,  $J_a$  is set back to  $J_1$  and section  $b$  is pumped with  $J_b = J_k$ . The output spectrum

$$I_{bk} = I_{ref} \exp[-\alpha(J_k)L_b] + I_{b,spont}(J_k)$$

is then measured and the absorption coefficient for each wavelength relative to the reference level gain is calculated from the formula

$$\alpha(J_k) = -\frac{1}{L_b} \ln \left[ \frac{I_{bk} - I_{b,spont}(J_k)}{I_{ref}} \right]$$

where  $I_{b,spont}(J_k)$  is found by setting  $J_a = 0$  and  $J_b = J_k$  and measuring the output spectrum. The absorption spectra are also measured for various reverse bias levels ( $E_b$ ) applied to section  $b$ , but here no spontaneous emission component is present from section  $b$ , so in this case

$$\alpha(E_b) = -\frac{1}{L_b} \ln \left[ \frac{I_{bk}}{I_{ref}} \right]$$

Only the current through the sections is altered during the experiment and we can assume that the optical coupling to the spectrum analyser remains constant which means that the spectra are comparable. The spectra are measured using an Advantest spectrum analyser and the data are collected and then processed by a computer.

**Results:** The results presented here were obtained with a laser wafer and fabrication method which are fully described in [3, 4]. Briefly, the laser wafer was a separately confined multi-quantum well material; the active layer was 200nm thick with four GaAs

quantum wells 10nm thick. The length of the long section (section  $a$  in Fig. 1) was 380 $\mu$ m, the short section (section  $b$  in Fig. 1) was 10 $\mu$ m long; there is a 1 $\mu$ m gap between sections and the ridge width is 3 $\mu$ m. In calibrating the spectra and calculating current densities no account is taken of current spreading; this tends to give over-estimates of the absorption and gain coefficients and current densities. An important consideration if these spectra are to be compared quantitatively with theory and other experimental measurements is the overlap factor,  $\Gamma$ , because the technique measures net modal absorption. The overlap factor, in a first order approach, can be taken as the ratio of total quantum well width to active layer width which gives  $\Gamma = 0.2$ , this will tend to be an over estimate.

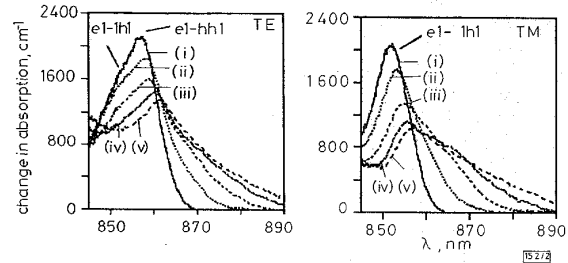


Fig. 2 Reverse bias absorption spectra for TE and TM polarisation showing broadening and shifting to higher wavelength of light-hole and heavy-hole exciton absorption peaks with increasing applied field

Applied field  $E_b$  (k Vcm<sup>-1</sup>):

- (i) = 0
- (ii) = 37
- (iii) = 74
- (iv) = 111
- (v) = 148

Fig. 2 shows the absorption spectrum of section  $b$  for TE and TM polarisations under varying reverse bias conditions. Both sets of spectra show exciton features which shift to higher wavelength and broaden with increasing reverse bias. This behaviour is well known [5] although as far as we are aware this is first time it has been measured in laser material. In the TE spectrum the heavy-hole exciton peak has a shoulder on the short wavelength side which is caused by the light-hole exciton. In the TM spectrum only the light-hole exciton peak is in evidence.

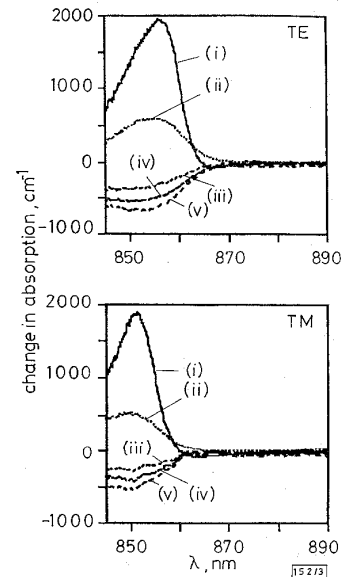


Fig. 3 Absorption spectra for TE and TM polarisation under forward bias conditions showing transition from absorption to gain as injection current density is increased

Applied  $J_b$  ( $J_1 = 5263$  Acm<sup>-2</sup>):

- (i) = 0
- (ii) = 0.5 $J_1$
- (iii) = 1.5 $J_1$
- (iv) = 2 $J_1$
- (v) = 2.5 $J_1$

Fig. 3 shows the absorption spectrum of section *b* for TE and TM polarisations under varying forward bias conditions. Both sets of spectra show that the exciton absorption peaks disappear as the forward bias is increased, and eventually gain (negative absorption coefficient) is apparent at forward bias current densities above  $5000 \text{ Acm}^{-2}$ . The TE spectra show higher gain than the TM spectra at a given current injection and the TM spectra are high at shorter wavelengths compared to the TE spectra. These observations are in accordance with theory as the TE spectra are dominated by heavy-hole transitions which have a higher density of states associated with them. The TM transitions are exclusively light-hole and are shifted to a shorter wavelength.

**Conclusions:** This Letter presents a simple technique for obtaining relative absorption and gain spectra of laser material. Compared to other techniques [7–9] it is relatively simple, and because it uses only small lengths of laser material it can operate with gains well above the normal threshold gain without gain saturation significantly perturbing the results. The complicated part of the method is preparing the two sectioned laser. It is limited to wavelengths close to the band edge although with more sophisticated signal processing it may be possible to extend the range of wavelengths. There are also some caveats about the calibration, the exact length of the measured section which has current injection is not known nor is the exact overlap factor.

The results obtained are at least in qualitative agreement with theory. The typical exciton broadening and shifting are observed in the reversed biased spectra, the polarisation behaviour is as expected from theory and the calibration is of the right order.

The measurement of the gain and absorption spectra provide a valuable insight into the operation of the laser and are of particular importance in modeling monolithic modelocking of semiconductor lasers because the effect of reverse bias can be directly compared to the gain.

**Acknowledgments:** The authors gratefully acknowledge the support of the EPSRC through grant number GR/H82471. The authors also are grateful for useful discussions with E. A. Avrutin and Joaquim Martins-Filho.

© IEE 1995  
Electronics Letters Online No: 19951483

13 October 1995

S.D. McDougall and C.N. Ironside (Department of Electronic and Electrical Engineering, University of Glasgow, Glasgow, G12 8LT, United Kingdom)

## References

- MARTINS-FILHO, J.F., IRONSIDE, C.N., and ROBERTS, J.S.: 'Quantum well AlGaAs/GaAs monolithic colliding pulse modelocked laser', *Electron. Lett.*, 1993, **29**, pp. 1135–1136
- MARTINS-FILHO, J.F., and IRONSIDE, C.N.: 'Multiple colliding pulse operation of a semiconductor laser', *Appl. Phys. Lett.*, 1994, **65**, pp. 1894–1896
- MARTINS-FILHO, J.F., AVRUTIN, E.A., IRONSIDE, C.N., and ROBERTS, J.S.: 'Monolithic multiple colliding pulse mode-locked quantum-well lasers: experiment and theory', *IEEE J. Sel. Topics Quantum Electron.*, 1995, **1**, pp. 539–551
- MARTINS-FILHO, J.F.: 'Monolithic colliding pulse mode-locked quantum well lasers', PhD Thesis, University of Glasgow, 1995
- HAYAKAWA, T., SUYAMA, T., TAKAHASHI, K., KONDO, M., YAMAOTO, S., and HUIKATA, T.: 'Polarization-dependent gain current relationship in (111)-oriented GaAs/AlGaAs quantum well lasers', *J. Appl. Phys.*, 1988, **64**, pp. 297–302
- ZORY, P.S. (Ed.): 'Quantum well lasers' (Academic Press, 1993), see Chaps. by CORZINE, S.W., *et al.*, and ENGELMANN, R.W.H., *et al.*
- HAKKI, B.W., and PAOLI, T.L.: 'Gain spectra in GaAs double heterostructure injection lasers', *J. Appl. Phys.*, 1975, **46**, pp. 1299–1306
- HENRY, C.H., LOGAN, R.A., and MERRITT, F.R.: 'Measurement of gain and absorption spectra in AlGaAs buried heterostructure lasers', *J. Appl. Phys.*, 1980, **51**, pp. 3042–3050
- BLOOD, P., KUCHARSKA, A.L., JACOBS, J.P., and GRIFFITHS, K.: 'Measurement and calculation of spontaneous recombination current and optical gain in GaAs-AlGaAs quantum-well structures', *J. Appl. Phys.*, 1991, **70**, pp. 1142–1156
- SCHMITT-RINK, S., CHEMLA, D.S., and MILLER, D.A.B.: 'Linear and nonlinear optical properties of semiconductor quantum wells', *Adv. Phys.*, 1989, **38**, pp. 89–188

## Single longitudinal mode ridge waveguide 1.3µm Fabry-Perot laser by modal perturbation

B. Corbett and D. McDonald

Indexing term: Semiconductor junction lasers

The authors introduce a cost effective technique which converts the multi-longitudinal mode output of a 1.3µm ridge waveguide Fabry-Perot laser into a single mode by creating modal perturbations along the length of the ridge. Up to 25dB side mode suppression is measured on their first lasers.

**Introduction:** A semiconductor laser emitting a single longitudinal and transverse mode has, among others, applications in optical sensing and wavelength division multiplexing. DFB/DBR technology can provide this laser but at the cost of additional growth, processing and associated yield. The simplest and cheapest fabrication technique for obtaining a single transverse mode is by etching a ridge waveguide in a Fabry-Perot (FP) cavity but this gain-guided structure tends to operate with multi-longitudinal modes. Single longitudinal mode emission has also been obtained with other device geometries such as external cavities, coupled sections [1] and by defining regular periodic perturbations along the ridge of a ridge waveguide [2].

It is known that scattering centres along the length of the FP cavity cause strong spectral perturbations [3]. Scattering centres at defined positions have been deliberately introduced into individual lasers using laser ablation [4, 5] or focussed ion beam etching [6, 7]. With defects at 1/2, 1/4 and 1/8 of the cavity length, multi-longitudinal mode emission has been converted into single longitudinal mode emission. In these experiments the defects are introduced into the cavity after laser fabrication. The defects extend through the active region thereby introducing a position dependent modulation of the gain.

In this Letter we precisely define the length of a 1.3µm FP laser during device fabrication by etching scribe channels. Slots are etched into the guide ridge with a controlled depth and location relative to the cavity length. The slots do not reach the active region of the laser but do cause modal perturbations at well defined positions along the length of the cavity. Optical frequencies that are resonant with any of the sub-section lengths are enhanced. The mode selection is caused by refraction of the mode on the scale of the cavity rather than by diffraction at the scale of the emission wavelength.

**Processing:** The layer structure is a conventional three layer active region consisting of a central 100nm thick bulk 1.3µm wavelength InGaAsP active layer cladded by 50nm of  $\lambda = 1.15\mu\text{m}$  InGaAsP. 4µm wide ridges are defined in the  $\langle 110 \rangle$  direction along with slots of 1µm length across the ridge. The slots correspond to positions of 1/2, 1/4 and 1/8 of the final cavity length. The ridge and slots are etched using  $\text{CH}_4/\text{H}_2$  reactive ion etching to 0.5µm of the top of the waveguide. Contact holes are opened in plasma deposited oxide to the top of the ridge. Following TiPtAu evaporation and alloy, scribe channels are defined perpendicular to the ridges at positions corresponding to the desired cavity length.  $\text{CH}_4/\text{H}_2$  is used to etch through the active layers. HCl is used to selectively etch the InP substrate and to define U channels thereby permitting cleaving of the chip into bars of precisely defined length. Self alignment can easily be introduced into the fabrication process. The chips are bonded with indium *p*-side down on copper headers and are tested CW.

**Characterisation:** L-I characteristics of uncoated 400µm long lasers with and without etched slots are comparable with a threshold current of 42mA at 22°C. The lasers emit in a single transverse mode. The spectra from the lasers are dramatically different. Fig. 1 presents spectra from the lasers at 70mA and 16°C. The conventional laser shows a typical multimode spectrum (Fig. 1*a*) while the slotted laser (Fig. 1*b*) is quasi single mode with a side mode suppression ratio (SMSR) of 25dB. There is a clear modulation of the spectrum at 8 full cavity modes. The emission wavelength is 8nm shorter in the slotted laser as also observed in [6].